Neutron spallation measurements and impacts on low-background experiments

E. Aguayo, R. T. Kouzes, and E. R. Siciliano

Phys. Rev. C **90**, 034607 — Published 10 September 2014

DOI: 10.1103/PhysRevC.90.034607

Neutron Spallation Measurements And Impacts On Low Background Experiments

E. Aguayo, R. T. Kouzes, E. R. Siciliano

Pacific Northwest National Laboratory, P.O. Box 999, Richland, WA 99352

PACS: 28.20.Cz, 28.20.Fc, 29.40.-n , 29.30.Hs, 96.50.S-

Keywords: neutron detection; ship effect; spallation; low background experiments; neutrinoless double beta decay

Ultra-low background experiments, such as neutrinoless double beta decay, solar neutrino, and dark matter searches, are carried out deep underground to escape background events created by cosmic ray muons passing through the detector volumes. However, such experiments may nevertheless be limited in sensitivity by cosmogenically induced backgrounds. This limit can be due to cosmogenically created radioactive isotopes produced either *in situ* during operation or prior to construction when the detector construction materials are above ground. An accurate knowledge of the production of the latter source of background is of paramount importance in order to be able to interpret the results of low-background experiments. One way to deal with the characterization of cosmogenic background production is to use Monte-Carlo simulations to model the spallation reactions arising from cosmic ray neutrons, protons and muons. The objective of this work was to evaluate the degree of accuracy that such simulations could provide by comparing measurements for various materials to results from two standard Monte-Carlo codes using the same physics model for generating intra-nuclear cascades. The simulated results from both codes provide the correct trends of neutron production with increasing material density. But, there was substantial disagreement between the models and experimental results for lower-density materials of Al, Fe and Cu. The model values, when normalized to the Pb experimental results, show disagreement with experiment by a factor of about two for Fe and Cu, and significantly greater for Al. It is concluded that additional neutron-induced spallation measurements are required to refine models routinely employed in underground physics research. Further data collection against the above materials is an initial list for benchmarking.

I. INTRODUCTION

Rare event searches based on observation of radioactive decay require ultra-low levels of backgrounds in order to probe physics with very low event rates. Solar neutrino experiments, neutrinoless double beta decay and dark matter searches are some of the physics experiments that expect event rates as low as a few per year [1]. The background-limited sensitivity goal of future neutrinoless double beta decay experiments is to probe effects with half-lives $>10^{27}$ years, equivalent to background rates of ~1 event/tonne-year [2, 3]. The key to rare event searches lies in the ability to characterize and reduce the background rate [4]. Cosmic ray primaries create showers in the atmosphere that include a broad spectrum of neutrons, protons and muons. One of the contributors to the intrinsic background rate is long-lived radionuclides that are induced by cosmic-ray secondaries [5, 6].

There are a few cases where an accurate knowledge of the exact contribution of the cosmogenically induced source of background may have a significant impact on the final result of an experiment. In particular, for germanium-based neutrinoless double-beta decay experiments, the radionuclides that have the potential to mask the low rate signal of interest in an energy range up to ~2.5 MeV are ^{60}Co (half-life of 5.27 years) and ^{68}Ge (half-life of 271 days). The latter is produced by cosmic ray secondaries in the range of 20-200 MeV when the detector materials are above ground, which is during manufacture and transport of germanium detectors. Its production is highly suppressed in underground environments where only a small muon flux is still present [7]. Thus, minimizing the time on the surface, and shielding of material when on the surface, is crucial to maintaining low experimental backgrounds [4]. Discrimination methods have been proposed by tagging on the ^{68}Ge daughter, ^{68}Ga, with a relatively long half-life (68 minutes), but no method has been proven to be fully successful in identifying events that are related to the decay of ^{68}Ge [8].

The reduction in production of ^{68}Ge through shielding and underground operation has been elaborated [9]. An accurate knowledge of the amount of ^{68}Ge in the detector material of germanium-based rare event experiments can have an impact in the interpretation of the results of the experiment and the likelihood of probing the desired physics with it. Modeling the mechanisms for the production of this, and other radionuclides of concern, is the approach used to estimate the limits to surface exposure for materials used in these experiments. In order to claim a degree of accuracy expected from modeling of the spallation process, a validation of such models against benchmark measurements must be carried out, with particular focus on the methods used to simulate the physics of intra-nuclear cascades (INC).

At the Earth's surface, the flux of muons (~168 $m^{-2}s^{-1}$ [10]) and neutrons (~134 $m^{-2}s^{-1}$ [11]) are comparable, while the proton flux (~2 $m^{-2}s^{-1}$ [12, 13, 14]) is smaller. The cosmic ray neutron component is the dominant source of the spallation-produced backgrounds discussed in this paper. Spallation events involve a cascade of neutron-induced interactions in a block of material, including interactions that cause nuclei to emit many nucleons. Muon interaction rates are down by about an order of magnitude compared to cosmic ray neutron and proton interactions at the Earth's surface. Simulations of spallation induced by cosmic rays, such as those by Martoff and Lewin [15], are based on parameterizations and extrapolations of cross sections such as those by Silberberg and Tsao [16, 17], resulting in significant model uncertainties.

The multiple neutrons produced in cosmic ray induced spallation events are often referred to as "ship effect" neutrons due to the observation of large numbers of neutrons produced in the vicinity of ships from the iron hulls acting as a spallation target [18]. The results of the investigation described here were a comparison between model and measurement of the number of neutrons escaping a target volume that resulted from spallation events induced by cosmic rays. Neutron multiplicity was measured, and modeled, for commonly used shielding materials (polyethylene, aluminum, steel, copper, lead and tungsten), and the results were compared.

The experimental measurements reported here were initiated to validate results from GEANT4 [19] Monte Carlo models to provide some confidence in the modeling results that have been used, for example, to predict the size of shielding needed on the surface of the Earth for reducing exposure of transported materials. The European ^{76}Ge neutrinoless double beta decay experiment (GERDA) has used Monte-Carlo simulations to design a transport shield, using ISABEL data and the SHIELD code [9]. The SHIELD result predicted an attenuation length for neutrons at 100 MeV in iron of about 240 g/cm^2 (0.30 m). Barabanov et al. predict that the transport shield design would reduce production of ^{68}Ge and ^{60}Co by 10 and 15, respectively. The GEANT4 model results performed for the MAJORANA DEMONSTRATOR [1] for this same transport shield disagreed with the Barabanov simulations using SHIELD by a factor of ~2.5 for the effect of iron as a shield material [20], with GEANT4 predicting a greater degree of shielding by the iron shield than the SHIELD code. That difference is what motivated the current experimental study.

When energetic neutrons interact with nuclei in a material, they can break apart one nucleus, releasing a large number of neutrons and other fragments that cascade through the material. A high efficiency neutron detector surrounding a block of material can thermalize and detect some fraction of these neutrons. The number of neutrons detected in a specified time window is referred to here as the "multiplicity." Recording the timing of each detected neutron can be used to generate a histogram of the measured multiplicity. For long enough time scales, much greater than the ~0.1 millisecond thermalization time for neutrons from a spallation event, the distribution will look random (Poisson). For short time scales comparable to the neutron thermalization time, high multiplicity events from the ship effect will show up in the multiplicity as a deviation from the

Poison distribution. One measure of this non-Poisson behavior is to count the number of events that exceed some multiplicity value (e.g., four or more), and such measures are used here to show the dependence of multiplicity on material type. It has been demonstrated previously that there is a strong dependence of multiplicity on material atomic mass; the current work provides a more controlled measurement than was previously reported [18].

The cosmic ray neutron spectrum follows approximately a E^{-1} dependence, and various authors have reported measurements [11, 21, 22, 23] with a fair amount of variation. The Gordon et al. results, being the most recent and extending over a wider range of energies, were used here. Since direct measurements of the effects of shielding on the cosmic ray neutron spectrum are not available, Monte Carlo modeling with GEANT4 has been used to compute such effects. However, there are large uncertainties (orders of magnitude) in the cosmic-ray neutron spectrum and the possible cross-section libraries used for such calculations. There are also large uncertainties in the neutron interaction cross-sections that directly impact the predictive ability of GEANT4 for cosmogenic production. The G4NDL4.0 cross-sections have been used for the GEANT4 calculations [20].

II. EXPERIMENTAL SETUP

The materials measured for cosmic ray induced neutron production rate included high-density polyethylene (HDPE), Al, Fe, Cu, Pb and W. The approach to the measurements was to use equal volumes and geometries (~30.5-cm cube, approximately one cubic foot) in order to eliminate corrections for geometry. This was possible for all measurements except for W, where a smaller volume was used due to the expense of obtaining a full volume of that material.

In the current study, a ^{3}He-based neutron coincidence counter [24] array was configured to measure neutron events induced by cosmic rays in the above target materials. The neutron coincidence counter used for the measurements consisted of an array of twelve ^{3}He tubes (0.95-m long, 0.05-m outer diameter, 4 atm.) in a HDPE moderator, as seen in Fig. 1 [25]. The four sets of tubes were configured to form a box with an inner cavity opening of 30.5 cm square, in a well detector fashion. The target materials were placed in the inner cavity on top of a 35.6 cm high wooden support so that they were in the vertical center of the detector array. The proportional counters were operated at 1200 V and were connected to three preamplifiers with their outputs or-ed together to conform a single transistor-transistor logic (TTL) output signal that was fed into a Versa Module Eurocard (VME) based analog to digital converter (ADC) manufactured by Struck Innovative Systeme (Hamburg, Germany) that generated a time stamp for each pulse from the ^{3}He tubes. The fast ADC allowed collecting multiplicity distribution information in a range from one to 80 counts in the gate width. Since the event rate was of order 10 Hz, dead time for the measurements was minimal. The system was designed to minimize electronic dead time between counts using a small but fast access memory where the data is logged for up to 80 consecutive counts, then the content of this first memory is transferred to the personal computer (PC). The dead time for a memory access in the first data tier is 150 ns, whereas the dead time for the Tier 1 memory transfer to the PC is 10 ms. Having these set dead times for memory access allows for a simple calculation to determine the dead time of the system.

From the acquired data, multiplicity was extracted in post-analysis using various coincidence-resolving windows (100 μs, 1 ms, 10 ms and 100 ms). The die-away time for the coincidence counter was ~50 μs, so the shortest analysis window was most appropriate.

The absolute efficiency (ε) of the coincidence counter was measured using a ^{252}Cf neutron source placed in the center of the detector system without target material in place. Data were accumulated with the VME system and with an ORTEC AMSR 150 (Oak Ridge, TN) shift register for comparison, both giving an efficiency for fission neutrons of 17%. The efficiency for the cosmogenic spallation neutron spectrum will differ from this value. Simulations discussed later indicate some variation in the efficiency with target material.

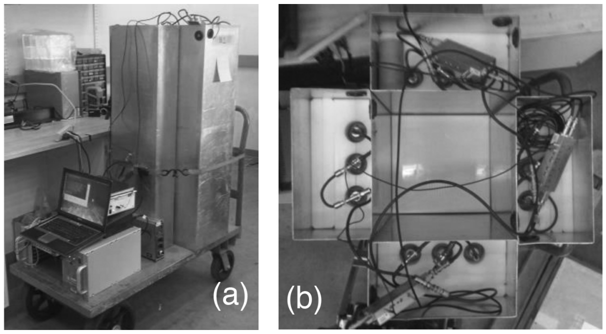

Fig. 1. Neutron counter system during data taking (a), and top view with HDPE in the target position (b).

III. EXPERIMENTAL MEASUREMENTS

All measurements were made at the 3440 Building at Pacific Northwest National Laboratory (PNNL). This location was selected due to the low overburden that it presents to the target material while still preserving indoor conditions. A portable muon counter [25] was placed by the counting system to monitor any fluctuations in the cosmic ray rate. The flux of muons during the experimental runs fluctuated at a level below 5%.

Measurements were made on all target materials to obtain at least 4×10^5 events, spanning times from 6 to 20 hours. The events were analyzed by counting the number of events in a time window and creating a histogram of these counts into a multiplicity distribution, and by performing an analysis using shift register logic (reals plus accidentals analysis). Information was extracted from the multiplicity distributions as the number of counts above the Poisson distribution, and the number of counts above a specific multiplicity. The analysis of background data showed agreement with a Poisson distribution, as expected, for all time analysis windows.

An example of the multiplicity distributions obtained from a Fe target where multiplicities over 16 were observed using a 100 μs window is shown in Fig. 2. The Poisson distribution in the figure, which is matched to the first channel of the data, shows the very non-Poisson nature of this multiplicity distribution.

For the case of W, the target size was much smaller than the other materials, and the data obtained was simply scaled by the volume of the W target compared to the other target materials, which all had the same geometry. In order to validate the assumption of linear dependence of neutron production rate with volume, a series of measurements were made with various volumes of Pb (ranging from 1000 cm^3 to 28000 cm^3). The result for both singles and doubles analysis of this data was a linear scaling of count rate with target volume, as shown in Fig. 3. GEANT4 models of these same dimensions were run, and also predicated a linear scaling of neutron rate with volume. Thus, it is reasonable to use linear volume scaling for the results of the W target measurements, as was done for the analysis described in this paper.

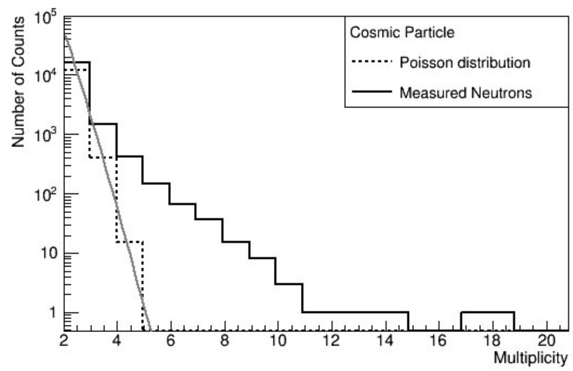

Fig. 2. Distribution of neutron multiplicity in a 100 μs time window caused by cosmic neutrons in Fe.

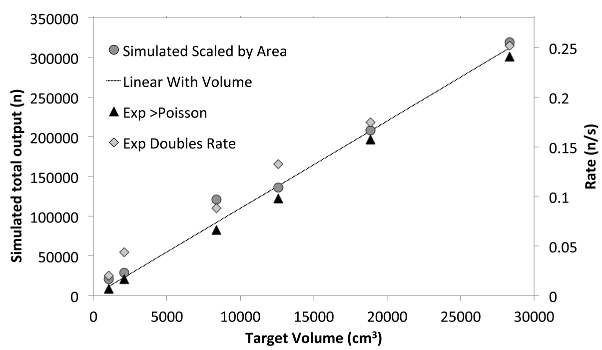

Fig. 3. Scaling of neutron rate with target volume of Pb.

A. Multiplicity Rate Results

One way to count multiplicity is to compare results from the various materials for a selected time window with events counted above a certain multiplicity value. Table 1 summarizes the data analysis runs using a 1 ms time window and multiplicity values of four or more, six or more, and eight or more. The table shows the density and neutron density for each of the materials, and the observed rate of events (in cps) for the fixed volume (approximately one cubic foot) of material used in the measurements, including scaling the tungsten results to this same volume. The general trend is increasing event rate with density, though the rate for tungsten (scaled by a volume factor of 9.1) is comparable to that of lead.

Table 1. Summary of experimental multiplicity results for a 1 ms time window.

Material	**Density (g/cm^3)**	**Target mass (kg)**	**Neutron Density (10^{24} n/cm^3)**	**Rate Mult. >4**	**Rate Mult. >6**	**Rate Mult. >8**
HDPE	0.95	28.05	0.25	0.0 ± 0.003	0.0 ± 0.0007	0.0 ± 0.0004
Al	2.7	76.8	0.84	0.0001 ± 0.003	0.0001 ± 0.0007	0. 0 ± 0.0004
Fe	7.87	222.6	2.54	0.019 ± 0.003	0.0042 ± 0.0007	0.0001 ± 0.0004
Cu	8.94	237.9	2.93	0.037 ± 0.003	0.0081 ± 0.0007	0.0029 ± 0.0004
Pb	11.3	320.1	4.11	0.220 ± 0.003	0.0760 ± 0.0007	0.0310 ± 0.0004
W	19.3	481.9	6.95	0.210 ± 0.003	0.0580 ± 0.0007	0.0220 ± 0.0004

These results can be compared with previous ship effect results measured at PNNL [18]. The previous measurements had included cement, Fe and Pb. While the trend in the new data reported here is the same as seen in the previous measurement, the current results are lower for Fe than previously observed. Because the systematic effects are better controlled in the new experiment, these new results are thought to be more representative of the actual effect since the earlier work used a different geometry for each material measured.

B. Analysis of Real and Accidental Events

An alternative method for extracting multiplicity information is to extract the neutron multiplicity from the data by performing an analysis using shift register logic, which is based on the assumption that the data contains a mixture of a "real" correlated distribution of neutrons (R) and an "accidental" (random background) distribution (A). This approach is referred to as "R+A" analysis. Analytical expressions for the factorial moments of the neutron multiplicity distribution were used in this multiplicity analysis. The extracted rates in this analysis are the singles rate (S, multiplicity = 1), doubles rate (D, multiplicity = 2), triples rate (T, multiplicity = 3) and quadruples rate (Q, multiplicity = 4), as detailed in [26]. In the data presented in this section, the duration of the window for the foreground multiplicity distribution (R+A gate) is 60 µs, and the background distribution is measured in a window of the same duration after a delay time interval (A gate) of 4 ms. These parameters were used since they were consistent with the empty detector die-away-time. No variation was made depending on target material, though that might affect the actual die-away-time. This analysis method is implemented in commercially available shift registers, such as the Canberra (Meriden, CT) JSR-14. In order to validate the implementation of this analysis method for the use in this work, a ^{252}Cf neutron source measurement was made and analyzed using the VME system and a JSR-14, with agreement to better than 20% in the doubles results.

Fig. 4 shows the measured multiplicity computed with the R+A method for the different materials studied in this work. A correlation between multiplicities larger than one and the material can be observed. Uncertainties are smaller than the markers other than for Al and HDPE for higher multiplicities. The data for the W sample had large uncertainties for all multiplicities in this R+A analysis, and are not shown.

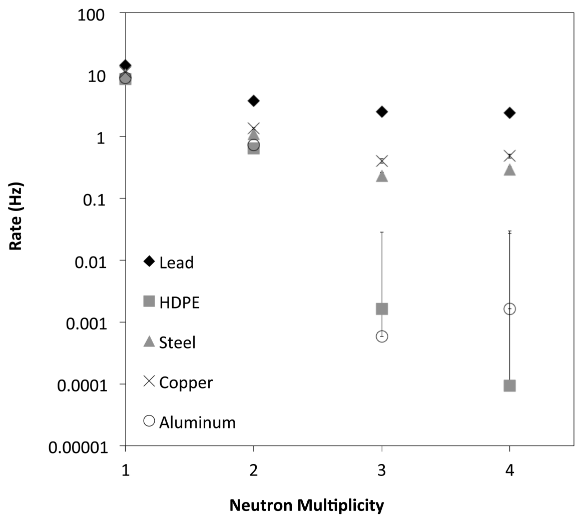

Fig. 4. Measured multiplicities for the different materials studied.

IV. SIMULATIONS

Both GEANT4 [27] and MCNPX [28] models were developed for comparison to each other and to the experimental results for the neutrons produced in the target materials by cosmic rays. The GEANT4 model was used to simulate aspects of the cosmic ray interactions including predicting outgoing neutron spectra and the multiplicity of the neutrons produced. The MCNPX model was used to make predictions that overlapped some of the GEANT4 results as well as to simulate the effects of the detector on the predicted neutron production. To minimize the possible causes of differences between the GEANT4 and MCNPX simulations, an effort was made for both to use the same cross-section libraries and physics model for intra-nuclear cascades.

A. GEANT4 Model Results

A GEANT4 Monte Carlo model was developed to compare to the measured experimental trend. The simulation makes use of the high precision (HP) neutron modeling capability, which is based on ENDF data (for information about ENDF see [29]) and the Bertini cascade physics model for higher interaction energies (up from 200 MeV [30, 31, 32]). The newer ENDF/B-VII.1 library was used for scattering data and better agreement with MCNPX modeling results was shown [33]. The simulated geometry matched the experimental geometry, which was exposed to the cosmic neutron flux.

The GEANT4 simulation was intended to evaluate the neutron physics within the code and therefore was kept very simple to avoid incorporating other effects, such as neutron detector efficiency, into the simulation. Thus, the model was to predict the relative response of materials, not the absolute response, as detailed in a previous report [34]. For the cosmic neutron spectrum at sea level, the model results utilize the Gordon et al. [11] parameterization of the cosmic ray shower, though a comparison with other spectra was also made. There are some differences in the shape of the incoming neutron spectrum at the Earth's surface from different measurements and models. The GEANT4 model was run for the Cu and Pb targets for three different neutron spectra to see to what degree these differences affect the calculations [11, 23, 35]. The result indicated that the choice of neutron parameterization could be responsible for ~25% of the difference in the comparison between model and experiment, based on the variation seen in the ratio of Cu to Pb. This is one of the contributing factors to observed differences between models, and between models and experiment, though model predictions to this accuracy are adequate for shielding designs.

Using a simplistic geometry consisting of a cube of material, the cosmic neutron spectrum was simulated impinging on the cube vertically from above. The output data from the simulation was the total number of secondary neutrons leaving the volume (down to 10^{-10} MeV) generated from a primary neutron. The simulations ran for a total of 10^{5} events for each material (2-10 hour simulation runs). Fig. 5 shows the result of the simulation for multiplicity for the incident cosmic neutron spectrum on the materials measured. As can be seen in the figure, the secondary neutron multiplicity per cosmic event increases as a function of material density. For Tungsten, 94% of neutrons emitted have a multiplicity greater than four, while only 2% of HDPE neutrons have a multiplicity greater than four.

differences in the spectra has not been included in the analysis presented here.

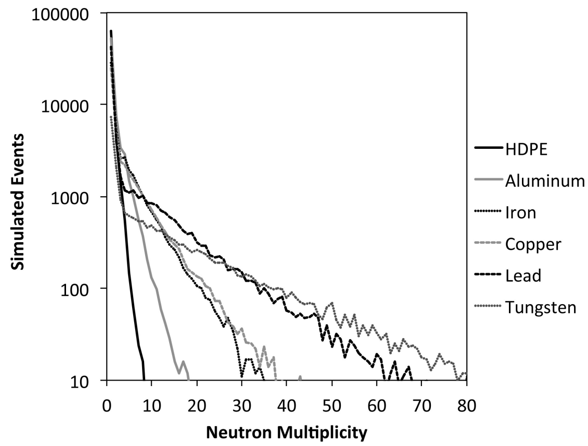

Fig. 5. GEANT4 simulated neutron multiplicity from sea-level cosmic-ray showers in the different materials studied.

The GEANT4 results for total outgoing neutrons (down to 10^{-10} MeV) for each material for 10^5 incoming neutrons with a cosmic ray distribution are shown as a function of material neutron density in Fig. 6. The materials with square markers are the ones that were also measured, while the diamond markers are computed results for other possible materials. Hydrogenous and low Z materials (water, HDPE) fall in the lower left corner of the plot, representing the lowest neutron yield, whereas lead and tungsten show the highest yield of neutrons from the materials studied. The models predict a generally linear dependence of neutron yield with neutron density, as indicated by the trend line (limited to those materials that were measured). Such factors as the dependence on nuclear shell structures in the model have not been studied. Similar trends are seen for multiplicities greater than six and eight, so the specific analysis method is not crucial to the trend that is observed in the modeling results. These models predict an experimental rate from one to seven detections per second at sea level, depending on the target material.

The GEANT4 model only went as far as determining the neutron flux leaving the cube of material and ignored any subsequent interactions in the detector or environment. Fig. 7 shows the computed spectra for neutrons exiting each of the materials. The detector is most sensitive to neutrons below one MeV, where these spectra are somewhat similar in shape. The impact of any

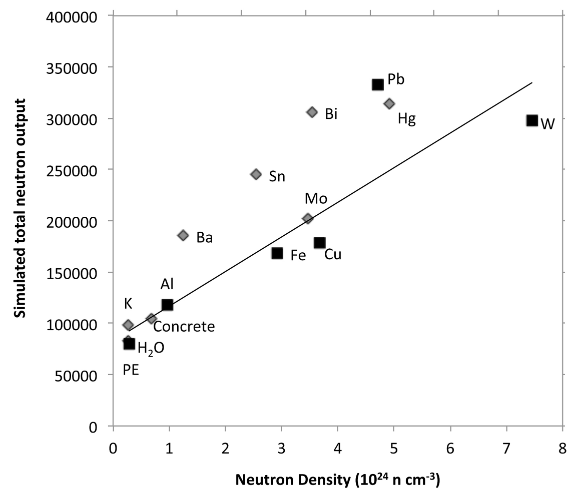

Fig. 6. Simulated neutrons out from a cube of material as a function of neutron density. The square symbols are for materials that were measured, and the trendline is for these measured materials.

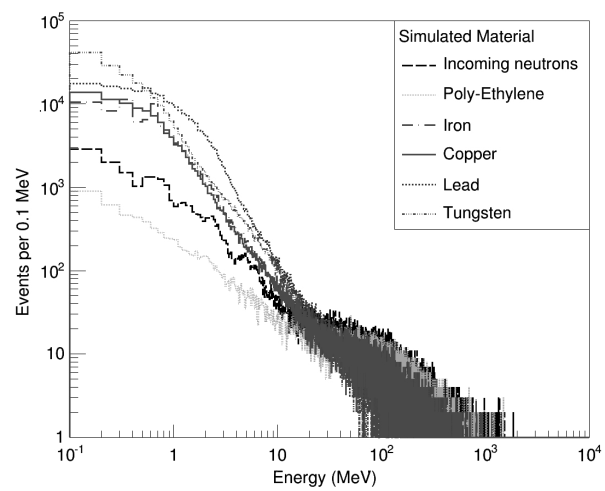

Fig. 7. Spectra computed with GEANT4 for neutrons exiting each of the materials.

B. MCNPX Monte Carlo Model Results

As a comparison to the GEANT4 simulation results, a model was created using version 2.70 of the Monte-Carlo code MCNPX [28] of the cubes of materials, and responses were calculated to cosmic neutrons, protons and muons. In each case, a 30.8 cm by 30.8 cm square, downward-directed "beam" of particles was incident on the cube of material, and the neutrons leaving all sides of the cube were tallied. The extended capability of MCNPX provides a large number of physics models for use above the (20~150 MeV) limits in the tabulated cross-section data. One high-energy application for which the physics models were developed in MCNPX was for the design of spallation targets for proton accelerators. Although comparisons (and thus validation) of some of those physics models were for mono-energetic proton beams, it was assumed they would also be applicable for the cosmic-neutron induced spallation results reported here.

In MCNPX, the calculation of nuclear spallation above the tabulated cross-section data limits is performed in three stages: INC, evaporation, and gamma ray decay. The INC stage involves elastic and non-elastic nuclear scattering and, if at high-enough energies, their emission of high-energy particles and light ions. At lower energies the INC stage uses a pre-equilibrium model for the transition from the first reaction to "equilibrium," where all particles are below a threshold for direct particle production. Then, the residual nuclei "evaporate" neutrons, protons, light ions, via fission, etc., followed in the last stage by gamma rays. The evaluation in MCNPX of the above processes is done via the Los Alamos High-Energy Transport module, LAHET, [36, 37]. For the targets and energies evaluated in this study, 10^6 source neutrons were used, and neutrons, protons, and charged pions were the primary particles transported. To compare the MCNPX results to the GEANT4 results, the (default) Bertini INC model, as implemented in the LAHET module, was used for all the MCNPX results reported here.

Simulations were run for monoenergetic neutrons (1 MeV, 10 MeV, 100 MeV, and 1 GeV) incident on cubes of the various materials. Table 2 provides the ratio of outgoing neutrons to incoming neutrons for the cosmic spectrum and for each of these monoenergetic beams for the Pb cube. It is seen that for the lowest energy (1 MeV), neutrons are scattered but produce no net increase in neutrons, as expected due to the reaction energies required to produce secondary reactions. At 10 MeV, there are a few net excess neutrons, likely due to elastic scattering. The 100 MeV and 1 GeV results show an increasing cascade process occurring. At 1 GeV, about 27 neutrons are produced on average for every incoming neutron. The cosmic-ray spectrum flux produces an average of 2.4 neutrons per incident neutron in Pb. The table also shows a comparison to the GEANT4 results, where available. It is seen that the MCNPX and GEANT4 results show some variance (from 7% to 27% difference). This provides some confidence that the two modeling approaches are giving results consistent to this level.

Table 2. Ratio of outgoing neutrons to incoming neutrons for Pb cube.

Neutron Energy (MeV)	MCNPX Ratio of Outgoing Neutrons to Incoming Neutrons	GEANT4 Ratio of Outgoing Neutrons to Incoming Neutrons	Percent Difference GEANT4 -MCNPX
Cosmic Flux	2.4	3.3	27%
1	1.0	0.8	-25%
10	1.4	1.5	7%
50	3.8	-	-
100	5.6	7.2	22%
200	8.7	-	-
600	13	-	-
800	22	-	-
1000	27	30	10%
1200	30	-	-

Another result of the MCNPX model was to predict the number of incoming neutrons that had no interactions (i.e., not scattered) during their passage through the cube of material. It was found that only the high-energy neutrons have a small probability of not interacting in the cube of material. Over 90% of the cosmic flux interacts at least once in all materials, with 9% not scattered in the cube of HDPE and only 0.04% not scattered in the W cube.

The MCNPX model was used to look at the neutron production from the neutron, proton and muon components of cosmic rays. Table 3 summarizes the results for the cosmic neutrons, protons and muon spectra entering the cube of material resulting in neutrons coming out of the cube of material. The data is presented in terms of per incident particle. Also shown for protons and muons are the numbers scaled to the relative fluxes of these particles to neutrons in the sea level cosmic-ray spectrum. The last column provides the percent contribution to the total number of outgoing neutrons from incident muons plus protons.

Table 3. MCNPX results for total neutrons out for cosmic ray components incident on various materials.

Material	Neutrons Out/ Neutrons In	Neutrons Out/ Protons In	Neutrons Out/ Muons In	Neutrons Out Scaled to Proton Flux	Neutrons Out Scaled to Muon Flux	% Contribution of Muons Plus Protons
HDPE	0.75	0.24	0.00	0.00	0.00	0.5%
Fe	1.35	3.34	0.11	0.05	0.14	12.1%
Cu	1.45	4.14	0.13	0.06	0.16	13.2%
Pb	2.36	9.47	0.22	0.13	0.28	14.6%
W	2.11	9.88	0.32	0.13	0.41	20.4%

The table shows that the incident cosmic-ray neutrons account for the bulk of the spallation events. The cosmic-ray protons contribute from 0.4% to 5.1% to the total number of outgoing neutrons depending on the material, with the largest contribution for the heaviest materials. The cosmic-ray muons contribute from 0.1% to 15% to the total number of outgoing neutrons depending on the material, with the largest contribution for the heaviest materials. Overall, protons and muons create up to 20.4% (for W) of the outgoing neutrons for the geometry studied here.

Shown in Fig. 8 is the comparison of the GEANT4 and MCNPX results for the total outgoing neutron fluence as a function of neutron density for the various materials. Both simulation approaches show a similar general trend, although there is a difference in the predicted total number of neutrons produced (~50% difference for Pb and W).

The MCNPX model was extended to include the detector assembly. This was done to determine the size of any detector-induced effects and their influence on the detected efficiency for the different materials. Fig. 9 shows the total number of neutrons exiting the material block with and without the detector as a function of atomic mass (A), normalized by the number of incident neutrons. The lines are to guide the eye, point-to-point.

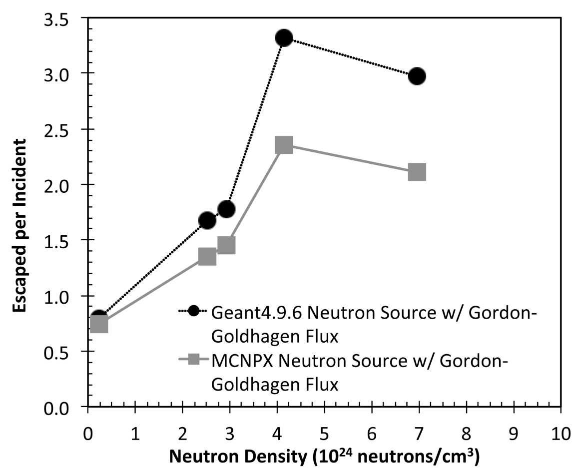

Fig. 8. MCNPX and GEANT4 results for total neutrons out for different materials.

The presence of the detector has a significant effect on the number of neutrons coming out of the target due to scattering of neutrons back into the target by the detector. The (normalized) line showing $A^{0.73}$ is the reported approximate cross section dependence given by Barabanov et al. [9]. The model results follow the general trend of this line, but have significant scatter. Percent detected is the number of neutrons detected by the detector divided by the number of neutrons incident on the target. The increase in percent detected with density is due to the multiplication in the dense materials.

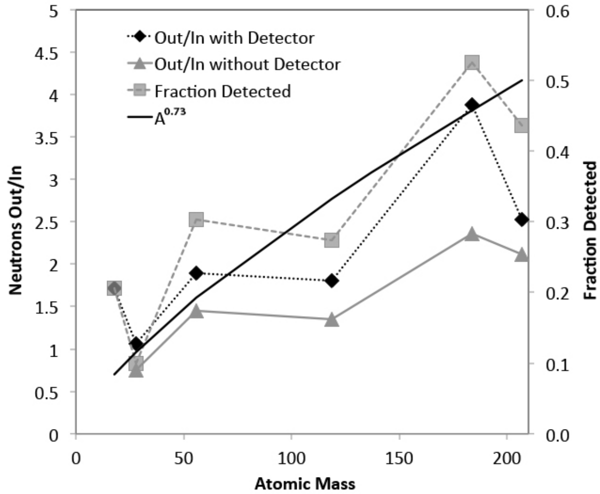

Fig. 9. MCNPX results versus atomic mass (A) for neutrons out and neutrons detected with or without the detector in place, normalized to the number of incident neutrons.

V. COMPARISON OF SIMULATED AND MEASURED RESULTS

Fig. 10 shows a direct comparison of the GEANT4 Monte Carlo model results (for net counts above a Poisson distribution) with the measurement results for net counts greater than the Poisson distribution, where the measurement data has been scaled to match the Pb model value, since the model scale is arbitrary. The 1 ms time window experimental data was used for the comparison, and the 0.1 ms data produces a similar result. The errors on the experimental values are smaller than the markers, while the GEANT4 model results show a 20% uncertainty. The HDPE model and measurement results are consistent, and the W experiment is also similar to the simulation. However, the Al, Fe and Cu results do not agree with the model, predicting a higher rate by about a factor of two to three for Cu and Fe, and a factor of 25 for Al.

The direct absolute comparison between the model and experiment is complicated since detection efficiency has not been taken into account as a function of multiplicity. The detection "efficiency" for the model is 100%, whereas the detection efficiency for the experiment is only ~17% for each neutron. Thus, a correction factor has to be applied to the experimental data (or the model results) based on the theoretical detection efficiency. This correction factor must take into account the efficiency for detecting the number of neutrons that are available to detect. The comparison shown in Fig. 10 does not include such a material dependent correction.

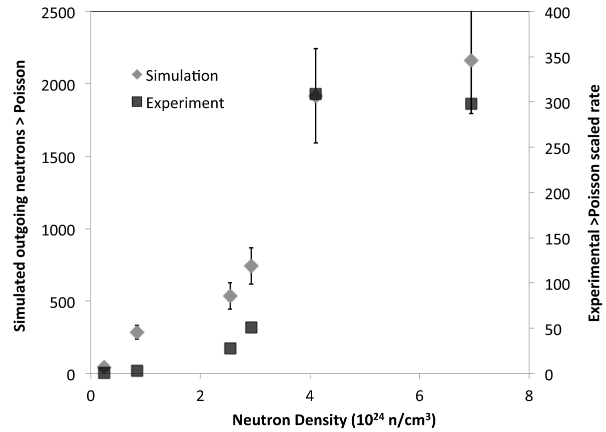

Fig. 10. Comparison of simulation to measurement for counts greater than Poisson in a 1 ms window.

Fig. 11 shows another comparison to simulation of the measured multiplicity found with the R+A analysis method, as discussed earlier, for the materials studied in this work as a function of neutron density. The experimental triples and quads from the R+A analysis are compared to the simulation of counts greater than a Poisson distribution, showing a similar trend with neutron density. The tungsten data was scaled by volume to be comparable to the other materials. The comparison using this method shows agreement for W and Pb, but again, the Fe and Cu experimental values are about a factor of two lower than the simulation, and Al and polyethylene did not yield any significant experimental results above zero even though the model predicts some.

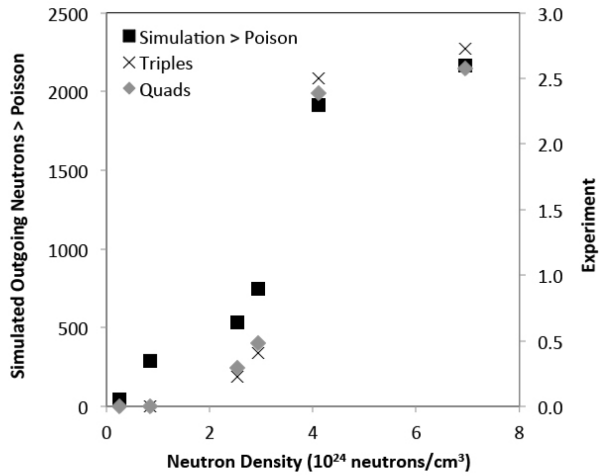

Fig. 11. Comparison of R+A analysis of measurements to simulation of counts greater than Poisson in a 1 ms window.

Without modifications to the source code, MCNPX has no option for simulating comparable multiplicity results. Since, however, all results from both codes that were comparable were in good agreement, it is assumed that the trend displayed by the above GEANT4 multiplicity results would be similar to MCNPX multiplicity results, if available.

These results for multiplicity indicate that there is a discrepancy between the model results and the measurements for the lighter materials. Compared at face value, a discrepancy exists. It is not clear how the measurement apparatus could produce a systematic variation in the manner seen. With regard to the model, there are several possible explanations: the incoming neutron spectrum might be different than assumed, the cross-section libraries (typically available for energies below ~150 MeV) might be insufficient between materials, or more likely, the use of the Bertini model for simulating the INC process might cause the observed differences. This focus on the Bertini model as being the most likely cause derives from a recent comprehensive study by Mashnik & Kerby [38] and references therein, where they compare a large body of proton-beam induced fragmentation data from light targets to the using the Cascade-Exciton Model (CEM03.03) implemented in the MCNP6.1 replacement to MCNPX. Those results show very good agreement (better than factors of 2) with all the targets including aluminum. Since fragmentation comparisons are a more rigorous test of physics models than multiplicity data, and if the Coulomb effect differences between the incident nucleons can be ignored, then using the CEM03.03 model may resolve the discrepancies reported here.

The origin of this discrepancy requires further investigation: is there a problem with the measurements or with the models? If this disagreement is correct, the model over-predicts the interaction rate for lower density materials (Al, Fe, and Cu), and thus the effectiveness of iron and copper shielding on the incoming neutrons could be substantially smaller than currently assumed.

The development of proton-beam-induced spallation targets for neutron source facilities has developed a good basis for heavy target production rates used in the simulations; however, lighter materials like aluminum, iron and copper may not have validated cross sections for the cosmic energies studied here. Publications on spallation production from these light nuclei are limited and not directly applicable to the energies of interest here [38, 39, 40, 41, 42]. The reported disagreement between data and models is often a factor of two. Experimental measurements of neutron energy spectra exiting thick targets of these materials should be made with incident spectra similar to that from cosmic rays in order to provide more information directly applicable to the observed discrepancy.

VI. CONCLUSIONS

This paper has reported on multiplicity measurements induced by cosmic rays at the Earth's surface for a range of materials and compared them to Monte-Carlo modeled results based on the GEANT4 and MCNPX simulation codes. Measurements of neutron multiplicity were performed using a neutron coincidence counter for HDPE, Al, Fe, Cu, Pb and W.

The evaluation reported here was undertaken to study the degree of accuracy expected when using two different Monte Carlo models to simulate spallation neutron yields from different shielding materials induced by cosmic rays in the range of 20-200 MeV. This was motivated by the difference between shield model results from two different simulations that differ by a factor of ~2.5.

The result of this study is that the relative multiplicity per event extracted from the models are in agreement for dense materials, but disagree with the experimental findings by a factor of more than two for the lower density materials Al, Fe and Cu. The model over-predicts the effect of Fe shielding by about a factor of three. This might be an artifact of the way the neutron data was obtained, or it may represent limitations in the models for low-density materials.

Two Monte Carlo approaches, GEANT4 and MCNPX, were compared to each other to confirm the reproducibility of the experimental results with different independently developed codes. To the extent possible, the same cross-section libraries and INC models were used in both codes to minimize causes for them to differ. Several simulation runs involving mono-energetic neutrons in the range of interest for cosmic ray studies were performed and the result of the inter-code comparison is an agreement by better than ~30% in the total neutron yield.

The scope of this work was not to reproduce accurately the experimental set-up, but simply to evaluate the models' behavior when switching between different shielding materials. This result shows that the GEANT4 Monte Carlo model results follow the correct trend as determined by experiment for total neutron yield and multiplicity. The predicted multiplicity as a function of target material increased with material density, with an approximately linear relationship.

The MCNPX models showed that only a small percentage of the incident cosmic neutron flux is not scattered in a cube of target material. The MCNPX models also looked at the contributions from cosmic proton and muon secondaries on the Earth's surface. It was predicted that these two components could contribute 12% to the outgoing neutrons for iron, increasing up to 20% for tungsten, with the majority of neutrons being produced by cosmic ray neutrons.

These theoretical tools must be used with care to correctly simulate shielding techniques for the next generation of low-background experiments and to estimate background rates. Unless benchmark measurements are made to validate Monte Carlo modeling for each application, their use is limited to shielding comparison studies, not as a predictor of absolute shielding efficiency.

For a more direct tests and refinement of the models, future measurements should be performed using neutron beams that span the energies over the range of 20 to 200 MeV to produce neutron spectra exiting large volumes of materials. Results for a range of beam energies and especially the lower density materials would provide a greater level of confidence that the models could correctly predict the effects of such materials.

VII. ACKNOWLEDGEMENTS

The United States Department of Energy Office of Science Office of Nuclear Physics supported this work under grant DE-FG02-97ER41041. Pacific Northwest National Laboratory is operated for the United States Department of Energy by Battelle Memorial Institute under contract DE-AC05-76RL01830. The authors are grateful to Drs. Jason Detwiler, Azaree Lintereur, and Stepan Mashnik for helpful discussions about this work. PNNL-SA-101429.

VIII. REFERENCES

[1] CE Aalseth, et al. (MAJORANA collaboration). 2009. "The MAJORANA DEMONSTRATOR: An R&D project towards a tonne-scale germanium neutrinoless double-beta decay search." The American Institute of Physics, Conf. Proc. 1182, pp 88-91.

[2] SR Elliott, et al. (Majorana Collaboration). 2009. "The Majorana Project." J. Phys. Conf. Proc. 173, 012007.

[3] K-H Ackermann, et al. (GERDA Collaboration). 2013. "The GERDA experiment for the search of 0 nu beta beta decay in Ge-76." European Physical Journal C 73.

[4] JA Formaggio, CJ Martoff. 2004. "Backgrounds to Sensitive Experiments Underground." Ann. Rev. Nucl. Part. Sci. 54:361–412.

[5] M Marino, et al. 2007. "Validation of spallation neutron production and propagation within GEANT4." Nuclear Instruments and Methods in Physics Research A 582, pp. 611–620.

[6] DM Mei, ZB Yin, and SR Elliott. 2009. "Cosmogenic Production as a Background in Searching for Rare Physics Processes." Astroparticle Physics 31(6), pp. 417-420.

[7] L Pandola, M Bauer, K Kroninger, X Liu, C Tomei, S Belogurov, D Franco, A Klimenko, M

Knapp. 2007. Nuclear Instruments and Methods in Physics Research A 570, pp. 149–158.

[8] H Ejiri. 2005. "Double Beta Decay and Neutrino Masses." J. Phys. Soc. Japan 74, pp 2101-2127.

[9] I Barabanov, S Belogurov, L Bezrukov, A Denisov, V Kornoukhov, and N Sobolevsky. 2006. "Cosmogenic Activation of Germanium and Its Reduction for Low Background Experiments." Nuclear Instruments and Methods in Physics Research Section B: Beam Interactions with Materials and Atoms 251(1):115-20.

[10] KI Greisen. 1942. "The Intensities Of The Hard And Soft Components Of Cosmic Functions Of Altitude And Zenith Angle." Phys. Rev. 61, pp. 212-221.

[11] MS Gordon, P Goldhagen, KP Rodbell, TH Zabel, HHK Tang, JM Clem, and P Bailey. 2004. "Measurement of the Flux and Energy Spectrum of Cosmic-Ray Induced Neutrons on the Ground." IEEE Transactions On Nuclear Science, Vol. 51, No. 6; and private communication of data from P Goldhagen.

[12] IS Diggory, JR Hook, IA Jenkins, KE Turver. 1974. "Momentum Spectra Of Nuclear Active Particles In Cosmic-Radiation At Sea-Level. 1.Experimental-Data." Journal Of Physics A-Mathematical And General 7, Issue 6, pp. 741-764.

[13] PKF Grieder. 2001. "Cosmic Rays at Earth." Elsevier, Amsterdam.

[14] T Nakamura, Y Uwamino, T Ohkubo, A Hara. 1987. "Altitude Variation of Cosmic-Ray Neutrons." Health Physics, Vol. 53, pp. 509-517.

[15] CJ Martoff, PD Lewin. 1992." COSMO — a program to estimate spallation radioactivity produced in a pure substance by exposure to cosmic radiation on the earth." Computer Physics Communications 72, pp. 96-103.

[16] R Silberberg, CH Tsao. 1973. "Partial Cross-Sections in High-Energy Nuclear Reactions, and Astrophysical Applications, I. Targets With Z $\leq$ 28." Astrophysical Journal Supplement Series 220, 25, pp. 315-333.

[17] R Silberberg, CH Tsao. 1973. "Partial Cross-Sections in High-Energy Nuclear Reactions, and Astrophysical Applications, I. Targets Heavier Than Nickel." Astrophysical Journal Supplement Series 220, 25, pp. 335-368.

[18] RT Kouzes, JH Ely, A Seifert, ER Siciliano, DR Weier, LK Windsor. 2008. "Cosmic-Ray-Induced Ship-Effect Neutron Measurements And Implications For Cargo Scanning At Borders." Nuclear Instruments And Methods In Physics Research A 587, pp. 89-100.

[19] S Agostinelli, et al. 2003. "GEANT4-a Simulation Toolkit." Nuclear Instruments & Methods in Physics Research Section a-Accelerators Spectrometers Detectors and Associated Equipment 506(3), pp. 250-303.

[20] E Aguayo, RT Kouzes, JL Orrell, DJ Reid, JE Fast. 2012. "Optimization of the Transport Shield for Neutrinoless Double Beta-decay Enriched Germanium." Pacific Northwest National Laboratory Technical Report PNNL-21302, Richland, WA.

[21] TW Armstrong, KC Chandler, J Barish. 1973. "Calculations of Neutron Flux Spectra Induced in Earth's Atmosphere by Galactic Cosmic Ray." Journal of Geophysical Research 78, pp. 2715-2726.

[22] WN Hess, HW Patterson, R Wallace, EL Chupp. 1959. "Cosmic-Ray Neutron Energy Spectrum." Physical Review 116, pp 445-57.

[23] JF Ziegler. 1998. "Terrestrial Cosmic Ray Intensites." IBM Journal of Research and Development 42(1), pp. 117-139.

[24] T Switzer, RR Hansen, RT Kouzes, RJ Arthur, WK Pitts. 2003. "Neutron Detection Authentication Case Study." Pacific Northwest National Laboratory Technical Report PNNL-14222, Richland, WA.

[25] E Aguayo, JE Fast, RT Kouzes, JL Orrell. 2013. "The μ-Witness detector: A ruggedized, portable, flux meter for cosmogenic activation monitoring." IEEE Trans. Nucl. Sci. 60 689, pp. 689-692.

[26] N Ensslin, WC Harker, MS Krick, DG Langner, MM Pickrell and JE Stewart. 1998. "Application Guide to Neutron Multiplicity Counting." Los Alamos National Laboratory Technical Report LA-13422-M.

[27] GEANT4. 2011. The GEANT4 Collaboration. *Physics Lists - Use Cases*. Accessed on July 22, 2011 at

http://geant4.org/geant4/support/physicsLists/referencePL/useCases.shtml.

[28] DB Pelowitz (ed.). 2011. "MCNPX User's Manual," Version 2.7.0. Los Alamos National Laboratory Report LA-CP-11-00438.

[29] A Trkov, M Herman, DA Brown. 2009. "ENDF-6 Formats Manual." http://www.nndc.bnl.gov/csewg/docs/endf-manual-v7.pdf

[30] A Heikkinen, N. Stepanov and J.P. Wellisch. 2003. "Bertini intra-nuclear cascade implementation in GEANT4." arXiv:nucl-th/0306008v1

[31] HW Bertini. 1969. "Intranuclear-Cascade Calculation Of Secondary Nucleon Spectra From Nucleon-Nucleus Interactions In Energy Range 340 To 2900 MeV And Comparisons With Experiment." Phys. Rev. 188, p. 1711.

[32] A Boudard, J Cugnon, S Leray, C Volant. 2002. "Intranuclear cascade model for a comprehensive description of spallation reaction data." Physical Review C 66, 044615.

[33] D Wright. "GEANT4 Developments." AARM Meeting, 4 March 2013, SLAC, Stanford, CA.

[34] E Aguayo, RT Kouzes, AS Ankney, JL Orrell, TJ Berguson, and MD Troy. 2011. "Cosmic Ray Interactions in Shielding Materials." Pacific Northwest National Laboratory Technical Report PNNL-20693, Richland, WA.

[35] C Hagmann, D Lange, D Wright. 2008. "Cosmic-Ray Shower Library (CRY)." Technical Manual, 5 pages. Lawrence Livermore National Laboratory, Livermore, CA. http://nuclear.llnl.gov/simulation.

[36] RE Prael and H Lichtenstein. 1989. "Users Guide to LCS: The LAHET Code System." Los Alamos National Laboratory Report LA-UR-89-3014.

[37] RE Prael. 1994. "A Review of the Physics Models in the LAHET Code." Los Alamos National Laboratory Report LA-UR-94-1817.

[38] SG Mashnik and LM Kerby 2014, "MCNP6 fragmentation of light nuclei at intermediate energies." http://arxiv.org/abs/1404.7820v1,

Preprint submitted to Nuclear Instruments and Methods in Physics Research A May 1, 2014.

[39] W Amian, et al. 1986. "Experiments and theoretical investigations for a high-energy source shielding experiment at the Los Alamos WNR facility." Radiation Effects 96, p. 301-304.

[40] TB O'Hearn, AS Kumar, LR Greenwood. 1992. "Comparison of measured and calculated transmutation in copper at spallation neutron sources." Journal of Nuclear Materials 191-194, p. 1383-1386.

[41] K Ishibashi, et al. 1997. "Measurement of Neutron-Production Double-Differential Cross Sections for Nuclear Spallation Reaction Induced by 0.8, 1.5 and 3.0 GeV Protons." Journal of Nuclear Science and Technology 34, No. 6, p. 529-537.

[42] EJ Kim, et al. 1999. "Spallation Reactions for ^{59}Co and ^{nat}Cu at Incident Neutron Energies of 40 to 120 MeV." Journal of Nuclear Science and Technology 36, No. 1, p. 29-40.